Influence of Be-Doping on Electronic Structure and Optical Properties of ZnO*

Zheng Yongping[1], Chen Zhigao[1], Lu Yu[1], Wu Qingyun[1], Weng Zhenzhen[2], and Huang Zhigao[1,2,†]

(1 *Department of Physics, Fujian Normal University, Fuzhou* 350007, *China*)
(2 *Fujian Institute of Research on the Structure of Matter, Chinese Academy of Sciences, Fuzhou* 350002, *China*)

Abstract: The electronic structure and optical properties of $Zn_{1-x}Be_xO$ alloys were studied using first principle calculation based on density functional theory (DTF). The results indicate that the band gap of $Zn_{1-x}Be_xO$ alloys increases as Be composition increases. The major reason is that the valence band maximum (VBM) of O2p has no obvious shift while the conduction band minimum (CBM) of Zn4s shifts to higher energy as x composition increases. Calculated results of the imaginary part of the dielectric function reveal that the peak heights at 2.0 and 6.76eV decrease as x composition increases, which is attributed to the decrease of the Zn3d states after Be substitutes for Zn. Due to the increasing transition probability from VBM of O2p to CBM of Be2s in wurtzite structure BeO, the peak height at 9.9eV is enhanced and its position shifts toward higher energy.

Key words: ZnO; Be; electronic structure; optical properties; first principles
PACC: 7115A; 7115H; 4225B
CLC number: O472 **Document code**: A **Article ID**: 0253-4177(2008)12-2316-06

1 Introduction

ZnO is an oxide semiconductor and it has become interested topic due to its direct wide bandgap ($E_g \approx 3.3$eV), large exciton binding energy (~60mV) and high mobility (3.2×10^7cm/s). It has been considered as a next generation material used in the ultraviolet and visible optoelectronic devices and so on. To prepare ZnO-based optoelectronic devices, it is essential to fabricate high quality p-ZnO. Recently, some reports have shown that, using As and N as source of doping, one can get stable and reliable p-type ZnO [1]. It becomes more important for quantum control and energy band engineering to achieve ZnO-based quantum wells (QWs) and superlattice structures. This provides a good method to use the doped ZnO with a bandgap greater than pure ZnO as barrier layer of QWs structure. Ohtomo *et al*.[2] reported that doping Mg in ZnO can expand the bandgap. They also found that, as Mg content ($x \leqslant 0.33$) increases, the bandgap of $Zn_{1-x}Mg_xO$ alloys increases from 3.3 to 3.99eV, but further doping of Mg ($x > 0.33$) will lead to MgO phase segregates in the wurtzite $Zn_{1-x}Mg_xO$ lattice. Recently, $Zn_{1-x}Be_xO$ alloys have attracted significant interest because of their wider range bandgap modulation ability. Moreover, Ryu *et al*.[1,3,4] have prepared $Zn_{1-x}Be_xO$ films by hybrid beam deposition. The experimental results indicated that the concentration of Be varied over the entire range from 0% to 100% and no phase segregation between ZnO and BeO was detected. At the same time, they got ZnO-based ultraviolet light emitting diodes using BeZnO/ZnO as QWs. Ding *et al*.[4] and Kuo *et al*.[5] have studied the electronic structure of $Zn_{1-x}Be_xO$ alloys by *ab inito*. But few reports focus on studying $Zn_{1-x}Be_xO$ band gap alteration using the electronic structure combined with optical properties.

In this paper, the electronic structure and optical properties of $Zn_{1-x}Be_xO$ alloys are investigated using first principles method based on the density functional theory (DFT). Moreover, the change of the band gap and the influence of Be doping on the optical properties are analyzed.

2 Method and calculation

ZnO has hexagonal wurtzite structure and belongs to $P6_3mc$ space group with lattice constants $a = b = 0.325$nm, $c = 0.521$nm. We consider a $2\times2\times1$ supercell of $Zn_{1-x}Be_xO$ containing 16 atoms, and the Zn cations are replaced by Be cations, as shown in Fig. 1.

* Project supported by the National Natural Science Foundation of China (No. 60676055), the State Key Development Program for Basic Research of China (No. 2005CB623605), the Fund of National Engineering Research Center for Optoelectronic Crystalline Materials (No. 2005DC105003), and the Natural Science Foundation of Fujian Province (No. E0320002)

† Corresponding author. Email: zghuang@fjnu.edu.cn

Received 25 January 2008, revised manuscript received 10 August 2008

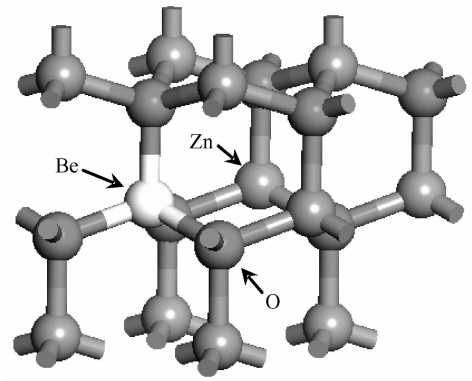

Fig. 1　$2\times2\times1$ supercell structure of $Zn_{1-x}Be_xO$ alloys

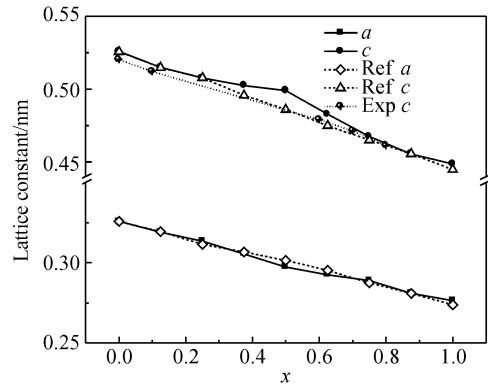

Fig. 2　x dependence of lattice constants a, c with geometry optimization for $Zn_{1-x}Be_xO$ alloys　The experiment and other calculated data are found in Refs. [1,7].

The electronic structure and optical properties were calculated using CASTEP code based on DFT[6]. A norm-conserving pseudopotential is used with Be ($2s^2$), O ($2s^2sp^4$), Zn ($3d^{10}4s^2$) as the valence-electron configuration for the beryllium, oxygen and zinc atoms, respectively, to describe the electron-ion interaction. The exchange-correlation potential was described using the generalized gradient approximation (GGA) of PBE scheme. Energy cutoff of plane-wave was set at 450eV where total energy converged to less than 1×10^{-6} eV/atom. Γ-centered $4\times4\times4$ k meshes were adopted to sample the Brillouin Zone for $2\times2\times1$ supercell. By change the number of doping beryllium from 0 to 8, we obtained $Zn_{1-x}Be_xO$ alloys with x = 0, 0.125, 0.25, 0.375, 0.5, 0.625, 0.75, 0.875 and 1 respectively.

3　Results and discussion

3.1　Structure optimization

The calculated lattice constants $a(x)$, $c(x)$ and bandgap value $E_g(x)$ are listed in Table 1 after geometric optimization. The x dependence of lattice constants a, c with geometry optimization for $Zn_{1-x}Be_xO$ alloys are also shown in Fig. 2. Table 1 and Figure 2 show that the lattice constants a, c decrease linearly as Be doping concentration increases due to smaller beryllium atom radius (0.14nm) than zinc atom radius (0.153nm). Calculated results are consistent with the experiment and other calculated results[1,7]. They also satisfy Vegard's law. However, there are three points deviating from Vegard's law for x = 0.375, 0.5, 0.625, which may result from various configurations in $Zn_{1-x}Be_xO$ alloys with these compositions[8]. In these compositions, the formation enthalpies are larger than the others and the variety ranges are also wider, indicating that these configurations are unstable. In the calculation, one of these configurations is adopted. Thus the deviation may exist. However, total change tendency is unchanged.

3.2　Bandgap E_g and state density

The bandgap E_g of $Zn_{1-x}Be_xO$ alloys as a function of beryllium composition x is shown in Fig. 3. Corresponding E_g values are listed in Table 1. This figure and Table 1 show that the bandgap E_g increases as Be composition increases. The bandgaps of $Zn_{1-x}Be_xO$ alloys can usually be described as a function of the beryllium composition x by

$$E_g(x) = xE_{g,BeO} + (1-x)E_{g,ZnO} - bx(1-x) \quad (1)$$

where $E_{g,BeO}$ and $E_{g,ZnO}$ are the bandgaps of BeO and ZnO, respectively, and b is the bandgap bowing parameter, being approximately took a constant. Based on the calculated E_g and by fitting the curve with Eq. (1), we can get that the bowing parameter b is about 5.926. But, the calculated values of $E_{g,ZnO}$ and $E_{g,BeO}$ deviate from the experiment ones, 3.3 and 10.6eV. Those deviations are contributed to the underestimation of the DFT theory for the bandgap calculation[9]. However, this will not influence the qualitative analysis. In order to investigate the reliability of the bowing parameter, we set the experimental values of ZnO bandgap (3.3eV) and BeO bandgap (10.6eV), and substituting the calculated bowing parameter b into Eq. (1), then plotting a new bandgap

Table 1　Calculated lattice constants $a(x)$, $c(x)$ and band gap value $E_g(x)$ after geometric optimization

x	0	0.125	0.25	0.375	0.5	0.625	0.75	0.875	1.0
a/nm	0.3256	0.3190	0.3134	0.3052	0.2972	0.2924	0.2889	0.2808	0.2764
c/nm	0.5256	0.5148	0.5076	0.5024	0.4990	0.4826	0.4675	0.4557	0.4487
E_g/eV	0.972	1.325	1.645	2.058	2.381	3.076	3.799	5.236	7.322

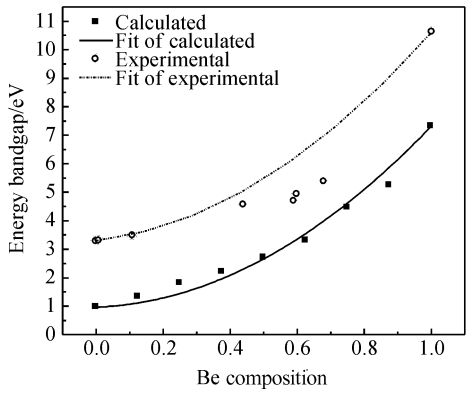

Fig. 3 Bandgap E_g of $Zn_{1-x}Be_xO$ alloys variety as a function of the beryllium composition x Here, the experimental data are found in Ref. [1].

energy curve to compare with the calculated ones. As shown in Fig. 3, although there exist some deviations between experiment results and new simulated curve, the change tendency still is consistent.

Figures 4 (a) and 4 (b) show the partial densities of states of ZnO and $Zn_{0.625}Be_{0.375}O$, respectively. From the figures, it is found that the valence band consists mainly of O2s, O2p and Zn3d orbitals. The O2s orbitals are located around −17eV with a band range of about 0.62eV, indicating that these states have been strongly confined and cannot interact with others. The O2p orbitals are predominantly found between −3.10 and 0.18eV in the uppermost valence band while the Zn3d orbitals with two peaks appear in the range from −6.55 to −3.10eV. The electron transition between Zn4s and O2p orbitals leads to slight movement of O partial state density to lower-energy band, indicating that ZnO is a metal-oxide semiconductor [10]. With the beryllium doping, the position of O2s orbitals does not change evidently but its band range increases slightly to 0.74eV. Although the Zn3d and O2p orbitals are all located in the valence band, the uppermost valence band are dominated by O2p orbitals. So, the valence band maximum (VBM) of $Zn_{1-x}Be_xO$ alloys is mainly determined by O2p orbitals. Moreover, the conduction band is mainly formed by Zn4s, Zn3p and Be2s.

Now, we further investigate the change of the bandgap by analyzing the partial density of states (PDOS) in different compositions x. Figure 5 shows the state densities of O2p, Zn4s, Zn3p and Be2s. This figure shows that, the uppermost valence bands of O2p orbitals do not change obviously; in the conduction band, the Be2s orbitals are enhanced with the increasing composition x and the positions of peaks for Zn4s, Zn3p and Be2s shift toward the higher energy. Moreover, it is clearly observed that the lowest conduction band which determines the conduction band

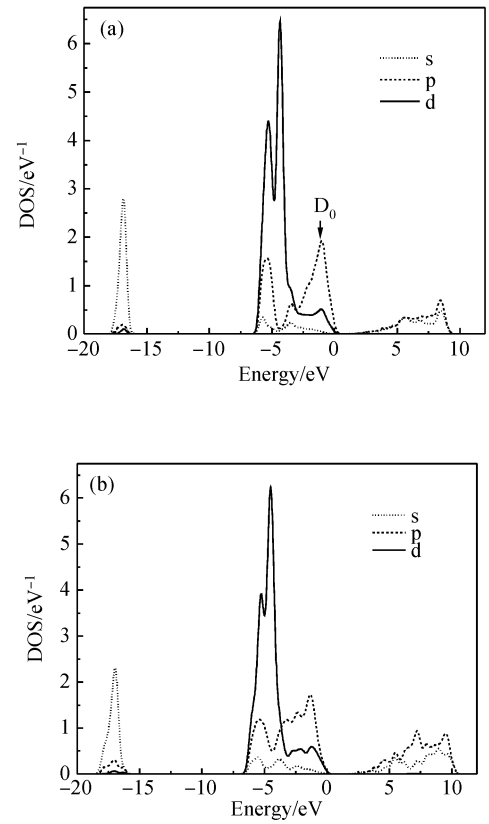

Fig. 4 Partial density of states for ZnO (a) and $Zn_{0.625}Be_{0.375}O$ (b)

minimum (CBM) is dominated by Zn4s orbitals. Therefore, it can be obtained that, the increase of the bandgap with increasing Be composition results from that, the CBM of Zn4s orbitals shifts toward the higher energy band. To explain this mechanism, the charge density difference of the $Zn_{1-x}Be_xO$ alloys is considered. Figure 6 shows the charge density difference of ZnO and $Zn_{0.875}Be_{0.125}O$ sliced cross the Zn—O and Be—O bonds in the same position. This figure shows that the offset of the electronic density from O atom to Be atom is larger than that from O atom to Zn atom after Be ion substitutes Zn ion. The density redistribution gives rise to the reduction of the electronic density of superposition of Zn and O atoms, the decrease of the bond energy and the increase of unit volume energy. As a result, the Zn4s orbitals shift toward the higher energy band and the corresponding bandgap is enlarged[11].

3.3 Optical properties

The macroscopically optical response function can be described in terms of dielectric function, $\varepsilon(\omega)=\varepsilon_1(\omega)+\varepsilon_2(\omega)$, where $\varepsilon_1(\omega)=n^2-k^2$, $\varepsilon_2(\omega)=2nk$. The imaginary part of the dielectric function $\varepsilon_2(\omega)$ can be calculated from the momentum matrix elements between the occupied and unoccupied wave functions within the selection rules, and the real part

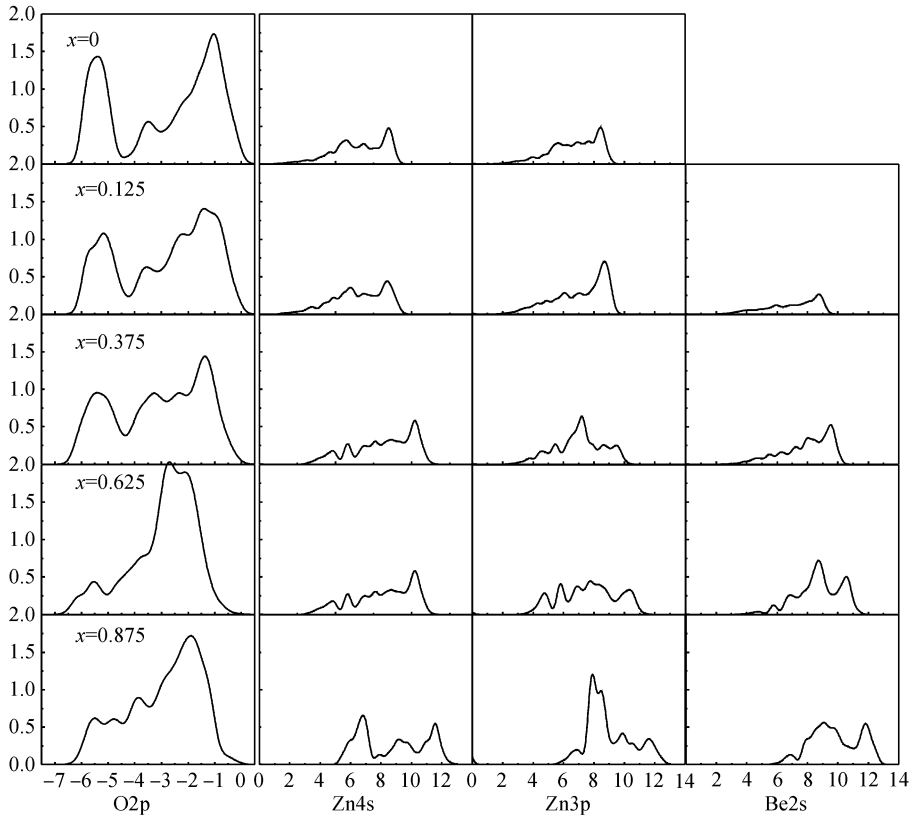

Fig. 5　Valence band of O2p and conduction bands of Zn4s, Zn3p, Be2s for $Zn_{1-x}Be_xO$ with different compositions x

$\varepsilon_1(\omega)$ of dielectric function can be evaluated from imaginary part $\varepsilon_2(\omega)$ by Krames-Kroning relationship. All the other optical constants can be derived from $\varepsilon_1(\omega)$ and $\varepsilon_2(\omega)$, such as reflectivity $R(\omega)$ and absorption coefficient $I(\omega)$[12].

$$\varepsilon_2 = \frac{4\pi^2}{m^2\omega^2}\sum_{V,C}\int_{BZ} d^3k\ \frac{2}{2\pi}\ |eM_{CV}(K)|^2 \times \delta[E_C(k) - E_V(k) - h\omega]$$

$$\varepsilon_1 = 1 + \frac{8\pi^2 e^2}{m^2}\sum_{V,C}\int_{BZ} d^3k\ \frac{2}{2\pi} \times \frac{|eM_{CV}(K)|^2}{[E_C(k) - E_V(k)]} \times \frac{h^3}{[E_C(K) - E_V(K)]^2 - h^2\omega^2}$$

$$I(\omega) = \sqrt{2}\omega[\sqrt{\varepsilon_1(\omega)^2 - \varepsilon_2(\omega)^2} - \varepsilon_1(\omega)]^{1/2}$$

$$R(\omega) = \frac{(n-1)^2 + k^2}{(n+1)^2 + k^2}$$

As we know, the imaginary part of dielectric function $\varepsilon_2(\omega)$ is the pandect of the optical properties for any materials. So the imaginary parts of the dielectric functions of the $Zn_{1-x}Be_xO$ alloys with $x = 0$, 0.25, 0.625, 1 as a function of the energy are shown in Fig. 7. This figure shows that, for a pure ZnO there are three peaks in the spectrum. The first peak I_1 at about 2.0eV comes mainly from the electron transition from the O2p upper valence band peak D_0 to Zn4s orbitals, as seen in Fig. 4. The transition between the Zn3d and O2p orbitals may lead to the

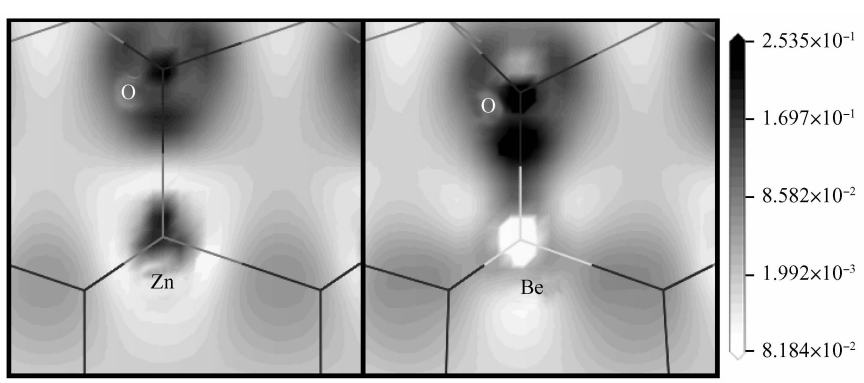

Fig. 6　Charge density difference of ZnO (a) and $Zn_{0.875}Be_{0.125}O$ (b) sliced cross the Zn—O and Be—O bonds in the same position　"Black" means to obtain electrons, and "White" means to loss electron.

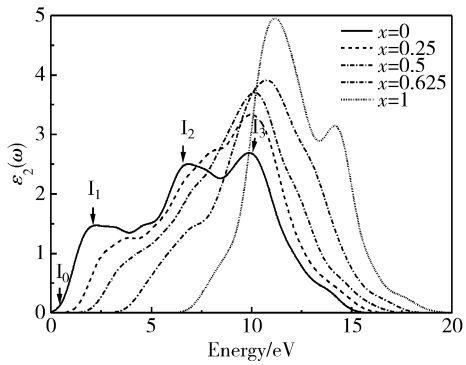

Fig. 7 Imaginary parts of the dielectric functions of the $Zn_{1-x}Be_xO$ alloys with different compositions x

second peak I_2 at about 6.76eV. And the third peak I_3 at 9.9eV is mainly derived from the transition between the Zn3d and O2s orbitals. There is a weak peak I_0 at about 0.94eV, which corresponds to band gap transition from Γ_9 to Γ_7[8]. It is also observed that, as Be doping increases, all these peaks shift toward the higher energy and the amplitudes of peak I_1 and I_2 trail off and disappear even, while the one of peak I_3 is enhanced gradually and its position shifts toward the higher energy. Shift in peak I_0 is the result of the enlarged bandgap energy E_g. The decrease of the amplitudes of peaks I_1 and I_2 results from Be substituting Zn gradually, reducing the transition probability from Zn3d to O2p. Moreover, the increase of Be composition can result in the formation of a wurtzite structure (B4) BeO, increasing the transition probability from valence band O2p to conduction band Be2s in BeO structure. Therefore, as Be composition increases, the intensity of peak I_3 increases gradually and its position shifts toward the higher energy [13].

4 Conclusion

The electronic structure and optical properties of $Zn_{1-x}Be_xO$ alloys have been investigated using *ab initio* calculations. The equilibrium lattice constants and bandgap E_g are presented. Calculated results indicate that, the $Zn_{1-x}Be_xO$ bandgap energy enlarges with the increasing of beryllium composition, which is due to the CBM of Zn4s orbitals shifting toward higher energy band. Calculation results of imaginary parts of the optical dielectric function also mean that, with increasing Be composition, the amplitudes of peak I_1 and I_2 decrease and disappear even. Moreover, with the addition of Be, the intensity of peak I_3 at 9.9eV is enhanced and its position shifts toward the higher energy, which is attributed to the formation of the wurtzite structure (B4) BeO and the increasing transition probability from valence band O2p to conduction band Be2s in BeO structure.

References

[1] Ryu Y R, Lee T S. Wide-band gap oxide alloy: BeZnO. Appl Phys Lett, 2006, 88: 052103

[2] Ohtomo A, Kawasaki M, Ohkubo I, et al. Structure and optical properties of ZnO/$Mg_{0.2}Zn_{0.8}O$ superlattices. Appl Phys Lett, 1999, 75: 980

[3] Ryu Y, Lee T S, Lubguban J A, et al. Next generation of oxide photonic devices: ZnO-based ultraviolet light emitting diodes. Appl Phys Lett, 2006, 88: 241108

[4] Kim W J, Leem J H, Han M S, et al. Crystalline properties of wide band gap BeZnO films. J Appl Phys, 2006, 99: 096104

[5] Han M S, Kim J H, Jeong T S, et al. Growth and optical properties of epitaxial $Be_xZn_{1-x}O$ alloy films. J Cryst Growth, 2007, 303: 506

[6] Segall M D, Lindan P J D, Probert M J, et al. First-principles simulation: ideas, illustrations and the CASTEP code. J Phys: Condensed Matter, 2002, 14: 2717

[7] Ding S F, Fan G H, Li S T, et al. Theoretical study of $Be_xZn_{1-x}O$ alloys. Physica B, 2007, 394: 127

[8] Fan X F, Zhu Z, Ong Y S, et al. A direct first principles study on the structure and electronic properties of $Be_xZn_{1-x}O$. Appl Phys Lett, 2007, 91: 121121

[9] Jaffe J E, Pandey R, Kunz A B. Electronic structure of the rock-salt-structure semiconductors ZnO and CdO. Phys Rev B, 1991, 43: 14030

[10] Zhang Fuchun, Deng Zhouhu, Yan Junfeng, et al. First-principles calculation of electronic structure and optical properties of ZnO. Acta Optica Sinica, 2006, 26(8): 1023 (in Chinese) [张富春, 邓周虎, 阎军锋, 等. ZnO 电子结构与光学性质的第一性原理计算. 光学学报, 2006, 26(8): 1023]

[11] Jin Xilian, Lou Shiyun, Kong Deguo, et al. Investigation on the broadening of band gap of wurtzite ZnO by Mg-doping. Acta Physica Sinica, 2006, 55(9): 4809 (in Chinese) [勒锡联, 娄世云, 孔德国, 等. Mg 掺杂 ZnO 所致的禁带宽度增大现象研究, 物理学报, 2006, 55(9): 4809]

[12] Shen Xuechu. Semiconductor spectrum and optical properties. 2nd ed. Beijing: Science Press, 1992 (in Chinese) [沈学础. 半导体光谱和光学性质. 第 2 版. 北京: 科学出版社, 1992]

[13] Amrani B, Hassan F E H, Akbarzadeh H. First-principles investigations of the ground-state and excited-state properties of BeO polymorphs. J Phys: Condensed Matter, 2007, 19: 436216

Be 掺杂对 ZnO 电子结构和光学性质的影响*

郑勇平[1]　陈志高[1]　卢　宇[1]　吴青云[1]　翁臻臻[2]　黄志高[1,2,†]

（1 福建师范大学物理系，福州　350007）
（2 中国科学院福建物质结构研究所，福州　350002）

摘要： 基于密度泛函理论(DFT)第一性原理计算了 $Zn_{1-x}Be_xO$ 化合物的电子结构和光学性质.计算结果表明 $Zn_{1-x}Be_xO$ 带隙随掺杂浓度的增加而变大.这种现象主要是由于价带顶 O2p 随掺杂量 x 的增加几乎保持不变,而 Zn4s 随掺杂量 x 的增加向高能端移动.光学介电函数虚部计算结果表明:在 2.0,6.76eV 位置随掺杂浓度的增加峰形逐渐消失,是由于 Be 替代 Zn 导致 Zn3d 电子态逐渐减少所致;而 9.9eV 峰形逐渐增强,是由于逐渐形成的纤锌矿结构 BeO 的价带 O2p 到导带 Be2s 的跃迁增加所致.

关键词： ZnO；Be；电子结构；光学性质；第一性原理
PACC：7115A；7115H；4225B
中图分类号： O472　　**文献标识码：** A　　**文章编号：** 0253-4177(2008)12-2316-06

* 国家自然科学基金(批准号:60676055),国家重点基础研究发展规划(批准号:2005CB623605),国家工程研究中心光电子晶体材料基金(批准号:2005DC105003)和福建省自然科学基金(批准号:E0320002)资助项目

† 通信作者.Email:zghuang@fjnu.edu.cn

2008-01-25 收到,2008-08-10 定稿